Coating of a textured solid

Jacopo Seiwert, Christophe Clanet, David Quéré

J. Fluid Mech. (2011), *vol.* 669, *pp.* 55–63.
doi:10.1017/S0022112010005951

Coating of a textured solid

JACOPO SEIWERT[1,2], CHRISTOPHE CLANET[1,2] AND DAVID QUÉRÉ[1,2]†

[1]Physique et Mécanique des Milieux Hétérogènes, UMR 7636 du CNRS, ESPCI, 75005 Paris, France
[2]Ladhyx, UMR 7646 du CNRS, École Polytechnique, 91128 Palaiseau CEDEX, France

(Received 14 September 2010; revised 21 October 2010; accepted 11 November 2010)

We discuss how a solid textured with well-defined micropillars entrains a film when extracted out of a bath of wetting liquid. At low withdrawal velocity V, it is shown experimentally that the film exactly fills the gap between the pillars; its thickness h_d is independent of V and corresponds to the pillar height h_p. At larger velocity, h_d slowly increases with V and tends towards the Landau–Levich–Derjaguin (LLD) thickness h_{LLD} observed on a flat solid. We model the entrainment by adapting the LLD theory to a double layer consisting of liquid trapped inside the texture and covered by a free film. This model allows us to understand quantitatively our different observations and to predict the transition between h_p and h_{LLD}.

Key words: coating, interfacial flows (free surface), lubrication theory

1. Introduction

Coating of solids is part of many industrial and daily-life processes such as painting, and it can be performed in various ways. One of the most common situations, the so-called dip-coating, consists of drawing the solid out of a bath. Ideally, the wetting liquid, of viscosity η and surface tension γ, is Newtonian, and the solid surface is flat and homogeneous. Withdrawing the surface at a constant speed V induces the deposition of a liquid film of constant thickness h_d. As shown by Landau & Levich (1942) and Derjaguin (1943), the film thickness can be calculated by balancing viscous forces responsible for the coating with capillary forces, which oppose it. This yields the Landau–Levich–Derjaguin (LLD) equation:

$$h_d \approx 0.94\, a\, Ca^{2/3}, \tag{1}$$

where $a = (\gamma/\rho g)^{1/2}$ is the capillary length of the liquid, and $Ca = \eta V/\gamma$ is the capillary number. Equation (1) is expected to be obeyed at small capillary numbers ($Ca < 0.01$). For capillary numbers larger than 0.01, the film becomes thinner than predicted by (1), owing to the action of gravity (Maleki *et al.* 2011). For silicon oils ($a = 1.5$ mm), this corresponds to films thicker than approximately 100 μm.

Most materials are not ideal, which generally impacts coating. For example, liquids may contain surfactants or be non-Newtonian, which modifies the entrained thickness (Ramdane & Quéré 1997; Shen *et al.* 2002; Afanasiev, Munch & Wagner *et al.* 2007). Even more commonly, solids are often porous (Aradian, Raphael & de Gennes 2000; Devauchelle, Josserand & Zaleski 2007), rough or textured, which affects the spreading and impregnation laws of liquid drops (Cazabat & Cohen-Stuart 1986; McHale *et al.*

† Email address for correspondence: david.quere@espci.fr

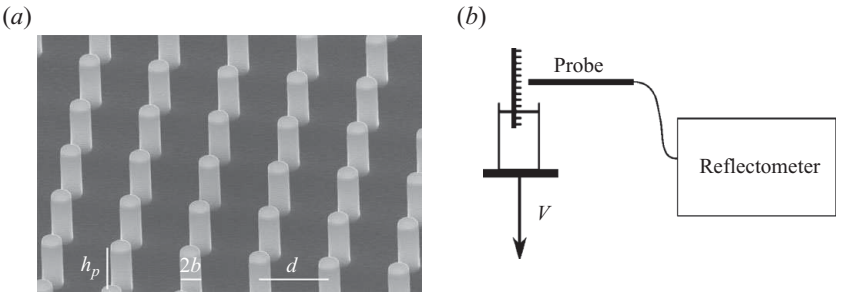

FIGURE 1. (*a*) Textured silicon surfaces obtained by etching silicon wafers and seen here by electron microscopy. For this sample, the spacing d between pillars is 10 μm, the pillar height h_p is 10 μm and the pillar diameter $2b$ is 3 μm, which yields a pillar density $\pi b^2/d^2$ of 7 %. (*b*) The experimental set-up consists of a hanging surface, a controlled stage to move the liquid bath at a constant speed V, and a reflectometer to measure the deposited film thickness. The probe both illuminates the sample with a spot (0.5 mm in diameter) of white light and collects the reflected light. The frequency spectrum shows oscillations due to the interferences produced by the liquid film (of known refractive index). By fitting the measured spectrum, we can determine the deposited thickness in the range of 0.5–60 μm.

2004; Courbin *et al.* 2007; Ishino *et al.* 2007; Savva, Kalliadasis & Pavliotis 2010). As for coating, it was reported by Chen (1986) and Krechetnikov & Homsy (2005) that the film deposited on a rough surface is always thicker than that on a smooth surface. Chen (1986) measured the thickness of films left behind after displacing a wetting liquid in a capillary tube (the so-called Bretherton 1961 configuration). He reported that the thickness at small capillary numbers tends to be independent of Ca, which he interpreted as arising from grooves on the tube walls. Krechetnikov & Homsy (2005) performed coating experiments on sanded surfaces in the roughness range of 0.1–1.5 μm. They anticipated a small-Ca regime of constant thickness, without observing it due to a microscopic roughness size. They also proposed to model the effect of roughness by a slip boundary condition at the top of the textures. We try here to overcome the difficulties of this problem by considering a well-defined model texture, consisting of pillars whose height is well above the resolution of the measurement. These characteristics allow us to provide observations in a large range of speed and viscosity, and to propose and test a model in the LLD regime, for $10^{-5} < Ca < 10^{-2}$, which corresponds to film thicknesses between 0.5 and 60 μm.

2. Experiments

Figure 1(*a*) shows a microscopic view of our surfaces, namely 2 cm × 2 cm silicon wafers decorated by square arrays of pillars of diameter $2b = 3$ μm kept constant in the study. Our fabrication technique (lithography and etching) allows us to vary both the spacing d between the pillars and their height h_p (Callies *et al.* 2005). Here we used surfaces with $d = 10$ or 20 μm, much smaller than the capillary length so that surface phenomena dominate the effect of gravity; h_p was varied from 1.4 to 35 μm.

The experimental set-up is sketched in figure 1(*b*). A bath of silicon oil is displaced at a constant speed V (1 μm s^{-1} < V < 10 mm s^{-1}) by a step-motor. Silicon oils totally wet the surfaces and their viscosity η can be taken in a large interval (here between 19 and 340 mPa s), keeping constant both the surface tension ($\gamma = 0.02$ N m^{-1}) and the density ($\rho = 960$ kg m^{-3}). The bath is first lifted up and the tested surface is immersed. Then it is withdrawn at a velocity V. The thickness h_d of the deposited film (defined

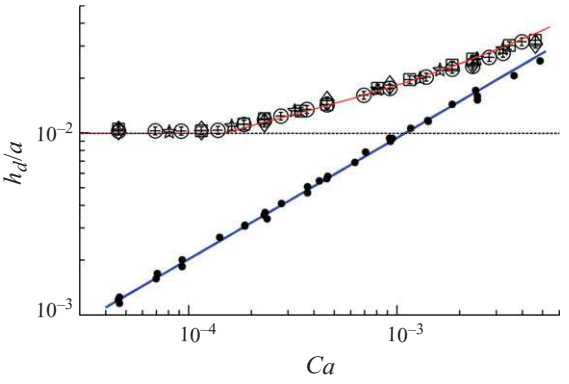

FIGURE 2. (Colour online) Deposited thickness h_d (normalized by the capillary length a) as a function of the capillary number $Ca = \eta V/\gamma$, for a plate decorated by pillars of height $h_p = 15\,\mu$m and mutual spacing $d = 10\,\mu$m (open symbols) and for a flat plate (full symbols). Symbols indicate the viscosity of the silicone oil: $\eta = 19$ (circles), 48 (squares), 97 (diamonds) and 340 mPa s (stars). The straight line represents the LLD law (1) and the horizontal dashed line shows the pillar height h_p. The line through the experimental data is a fit from the model discussed hereafter with $\alpha = 16.7$.

from the feet of the pillars) is measured by reflectometry, at the centre of the tested surface. This technique allows us to measure film thicknesses between 0.5 and 60 μm with uncertainties smaller than 5 %. Note that the pillars do not perturb the optical reflected signal, due to the modest surface fraction they occupy (5 %–10 %).

For a given surface ($h_p = 15\,\mu$m and $d = 10\,\mu$m) and silicon oils of different viscosities, we measured the deposited thickness h_d as a function of V. We plot these data in figure 2 by empty symbols, and compare with the behaviour obtained with a flat solid (bare silicon wafer, full symbols). While the latter data follow the LLD law (shown by a solid straight line), data for the textured surface collapse on the same curve, when plotted as a function of the capillary number $Ca = \eta V/\gamma$. At large Ca (high withdrawal speeds), the thickness tends towards the LLD law, as expected if the texture height h_p becomes negligible compared with the film thickness h_d. At low capillary numbers (small V), the film reaches a constant thickness h_{min} much larger than the thickness on a smooth surface.

In the plateau regime ($h_d = h_{min}$, dotted line), the liquid is not entrained by viscous forces, but trapped by capillarity within the pillar array. Thus, the quantity of liquid entrained in this regime no longer depends on either the withdrawal speed or on the oil viscosity. The minimum thickness h_{min} was extracted from plots such as figure 2, for different pillar heights h_p. It is shown in figure 3 to fit exactly this height.

We also observe in figure 2 that the transition between the two regimes, $h_d = h_p$ and $h_d = h_{LLD}$, extends over the range $10^{-4} < Ca < 10^{-2}$. In figure 4, we repeat the experiment for different pillar spacings ($d = 10\,\mu$m, squares and $d = 20\,\mu$m, circles), yet comparable height ($h_p = 9.8$ and $11\,\mu$m). The film in the transition regime is always thinner when the spacing is larger. This can be understood qualitatively: if the pillar density is lower, the effect of the texture is less pronounced and the film is closer to an LLD film.

Figure 4 also underlines two asymptotic situations. In the limit of high pillar density ($d \to 0$), the tops of the pillar array act as a quasi-continuous solid, so that an LLD film will be deposited on these tops, leading to a total thickness of $h_d = h_p + h_{LLD}$ (dotted line). Conversely, the solid line illustrates the case of highly dilute pillars ($d \to \infty$): at 'large' capillary numbers, pillars should hardly impact the LLD description, and

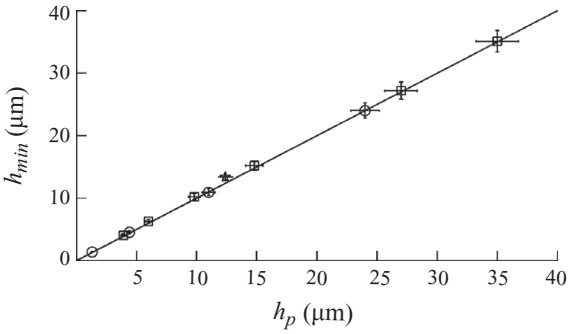

FIGURE 3. Minimum film thickness h_{min} as a function of pillar height h_p. Experiments are performed for two pillar densities: $d = 10$ μm (squares) and $d = 20$ μm (circles), and for $\eta = 19$ mPa s. The solid line represents $h_{min} = h_p$.

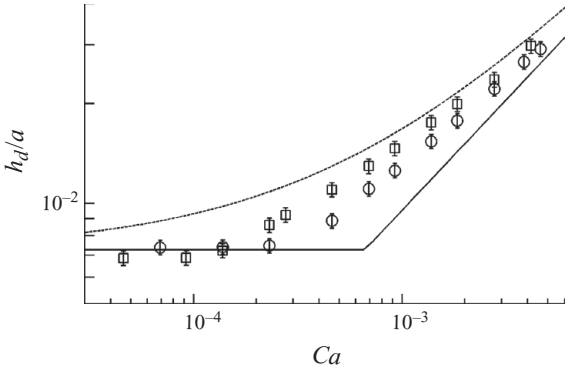

FIGURE 4. Deposited thickness as a function of Ca, for two different pillar spacings: $d = 10$ μm (squares) and $d = 20$ μm (circles), and comparable pillar height h_p (9.8 and 11 μm, respectively). We also represent two asymptotic behaviours: the low pillar density limit, $h_d = \max(h_p, h_{LLD})$ (solid line), and the high pillar density limit, $h_d = h_p + h_{LLD}$ (dotted line).

we expect (1) to be obeyed; at small Ca, pillars impose a minimum film thickness, provided they are close enough to trap the liquid by capillarity; hence, a thickness of $h_d = \max(h_p, h_{LLD})$, in this case (solid line). Experiments with different pillar spacings d (fixing the height h_p) all lie between these two asymptotic behaviours, and the thickness variations between both samples in figure 4 agree with this hierarchy: the smaller d, the larger h_d. In order to understand more quantitatively all these observations, we model the effect of the pillars by considering the two main properties they induce: (i) imposing a minimum film thickness and (ii) enhancing viscous friction at their surfaces.

3. The model

In the model (figure 5), the withdrawn film consists of two layers: a 'trapped' layer within the pillars of height h_p, and a 'free' layer of thickness $\delta(x)$ lying on top of the former.

In the trapped layer, we assume that the flow can be described by an 'apparent' viscosity $\eta_p = \alpha\eta$ larger than the actual liquid viscosity η. Indeed, in this trapped layer the friction takes place both on the 'ground surface' and on the pillars walls, which

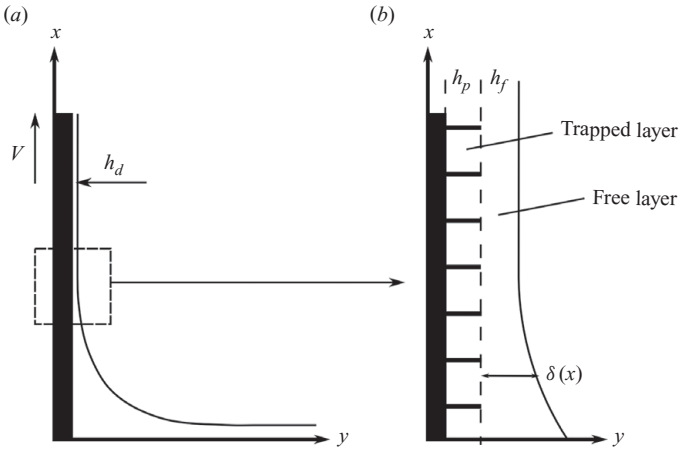

FIGURE 5. As a textured plate (in black) is withdrawn from a bath of wetting liquid along the x-direction, it draws a liquid film consisting of two layers: a trapped film of thickness h_p within the texture and a free film of thickness h_f above the latter. The total thickness entrained by the textured plate is $h_d = h_p + h_f$. The local thickness in the dynamic meniscus is denoted as $h(x) = h_p + \delta(x)$.

implies a viscous force scaling as $\eta V/h_p^2 + \eta V/d^2$ (Ishino *et al.* 2007). This is larger than the force $\eta V/h_p^2$ on a flat surface, which yields a scaling law for the factor α:

$$\alpha - 1 \sim \frac{h_p^2}{d^2}. \tag{1}$$

Hence, we expect for the factor α values between 1 (low pillar density or small pillars) and infinity (large pillar density or high pillars), depending on the design of the texture.

We propose to adapt the LLD theory to this two-layer system. The film consists of a flat entrained film of thickness h_d at large x (the coordinate along the plate), a static meniscus at the bottom, and a dynamic meniscus in between (Landau & Levich 1942; Derjaguin 1943). The dynamic meniscus, of thickness $h(x)$, is weakly bent ($h_x \ll 1$), which allows us to determine its shape in the lubrication approximation. It meets both the flat film (for $x \to \infty$: $h \to h_d$, $h_x \to 0$, $h_{xx} \to 0$) and the static meniscus, which selects the value of h_d for a set of parameters considered. As noted by LLD, gravity can be neglected for thin films ($Ca < 10^{-2}$). Inertia is also negligible, considering the low velocities, the viscosities and length scales involved. Hence, we get a parabolic profile for the velocity $v(y)$ in the film along the x-direction:

$$v = -\frac{\gamma\, h_{xxx}}{\eta_p}\frac{y^2}{2} + A_1 y + B_1, \quad \text{for } y < h_p, \tag{3a}$$

$$v = -\frac{\gamma\, h_{xxx}}{\eta}\frac{y^2}{2} + A_2 y + B_2, \quad \text{for } h_p < y < h. \tag{3b}$$

The four unknown constants A_1, B_1, A_2 and B_2 are determined by a set of four boundary conditions. (i) The non-slip condition at the solid plate ($y = 0$) imposes a velocity $v(0) = V$. (ii) The film is surrounded by air, so that we can neglect the tangential stress at the free surface: $\mathrm{d}v/\mathrm{d}y(y = h) = 0$. (iii) and (iv) Both the velocity and the stress are continuous at the boundary between the two fluid layers ($y = h_p$).

The total film thickness is equal to $h(x) = h_p + \delta(x)$, where h_p is constant and $\delta(x)$ tends towards the constant $h_f = \delta(\infty)$ in the flat film region. We finally express the conservation of flux Q (per unit width) between the dynamic meniscus and the film, which yields an equation for the thickness of the free layer δ:

$$Q = \frac{\gamma\, \delta_{xxx}}{3\,\alpha\eta}\left(\alpha\delta^3 + 3\delta^2 h_p + 3\delta h_p^2 + h_p^3\right) + (\delta + h_p)V = (h_f + h_p)V. \tag{4}$$

Note that this equation admits a solution of finite flux ($Q = h_p V$) for a free film of zero thickness ($h_f = 0$ and $\delta = 0$), contrasting with the LLD case. This corresponds to the plateau observed in figure 2. Introducing the dimensionless quantities $Y = \delta/h_f$ and $X = x/(h_f Ca^{-1/3})$, (4) can be rewritten as

$$Y_{XXX} = \frac{3\alpha(1-Y)}{\alpha Y^3 + 3\beta Y^2 + 3\beta^2 Y + \beta^3}, \tag{5a}$$

where we introduced a number β comparing the thickness of the entrained layers:

$$\beta = \frac{h_p}{h_f}. \tag{5b}$$

For $\beta = 0$, regardless of the value of α, and separately in the limit of $\alpha \to \infty$ regardless of the value of β, we recover the LLD description: we indeed expect an LLD film if there is no pillar ($\beta = 0$) or if the pillar array is so dense that it acts as a wall ($\alpha = \infty$). It is worth stressing the physical origin of each new term in (5*a*), compared to the LLD case ($\beta = 0$ in (5*a*)). If the influence of the sublayer was just treated by a slip boundary condition at the interface with the free film, i.e. a Joseph/Beavers-type condition (Beavers & Joseph 1967; Jäger & Mikelic 2000), we would only have the βY^2-term. The slip length here is found to be h_p/α, that is, the slip expected on a fluid layer of thickness h_p and viscosity η_p, as considered by Krechetnikov & Homsy (2005). However, we also find in (5*a*) two other terms ($3\beta^2 Y$ and β^3), which arise from the flow through the pillars. Equation (5*a*) indicates that this drainage will play an important role at large β, i.e. at small h_f, i.e. at low Ca, leading to a critical capillary number below which no free film is entrained, as discussed hereafter.

The LLD boundary conditions associated with (5*a*) are given by the matching with the flat film ($\delta(x) \to h_f$): at large X, Y tends towards 1, and Y_X and Y_{XX} both vanish. Conversely, the curvature Y_{XX} of the dynamic meniscus tends towards a constant as it approaches the bath (at large Y, Y_{XXX} tends to zero in (5*a*)) and thus can be matched with the curvature at the top of the static meniscus. As a main difference with the LLD theory, the non-dimensional shape of the meniscus here depends on the thickness (through the parameter β): its real shape is not universal and it cannot simply be found by rescaling a non-dimensional shape. The matching with the static meniscus has to be done numerically and it no longer leads to a power law. For a given value of α, h_f is deduced from the matching, from which we get the thickness $h_d = h_p + h_f$.

The resulting curve for $\alpha \approx 16.7$ is shown in figure 2, where it is observed to nicely describe the data. For each of the surfaces we tested, similar agreements were found, from which we deduced a corresponding value for α. The α obtained from these fits can be compared with the quantity expected from (2). In figure 6, we plot $\alpha - 1$ as a function of the square of the texture parameter h_p/d. The data follow a linear law in this plot, in agreement with (2), which confirms the key role of a 'viscous' trapped layer in the entrainment law. The slope in figure 6 is 7.2 ± 0.2. This value is related to the dissipation in arrays of pillars. For a liquid flowing among pillars of infinite

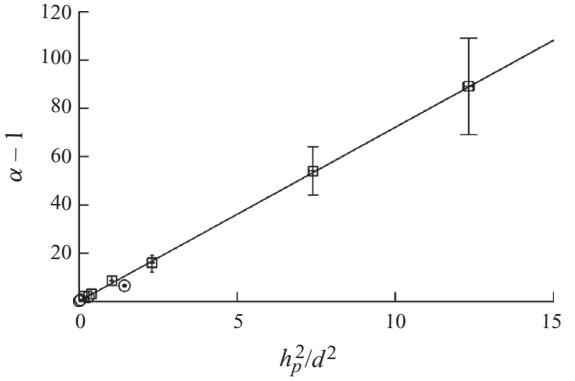

FIGURE 6. Value of the parameter α (deduced from fitting the experimental data $h_d(Ca)$ by our model), as a function of the texture parameter h_p^2/d^2 suggested by (2). Each data point corresponds to a series of withdrawals for a given textured plate, and the series of data is obtained by varying h_p and d (squares are for $d = 10$ μm and circles are for $d = 20$ μm). The solid line has a slope of 7.2.

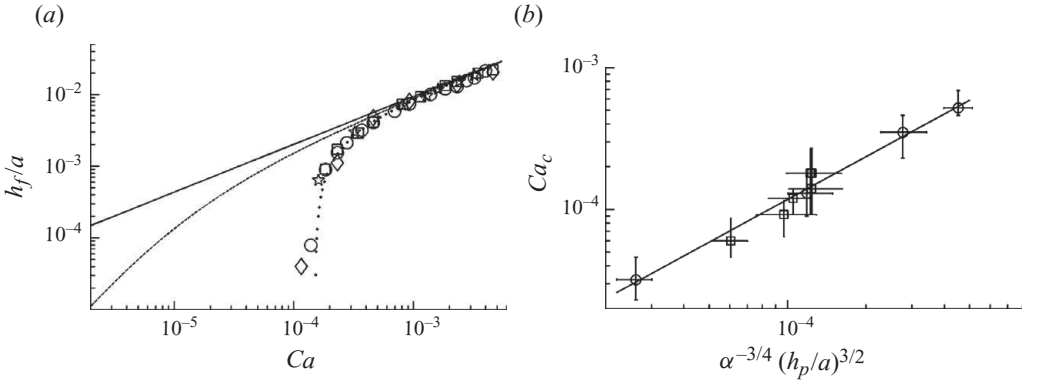

FIGURE 7. Influence of the flow inside the trapped layer: (*a*) thickness $h_f = h_d - h_p$ of the free film (data and symbols of figure 2), as a function of the capillary number. Here h_f is compared to the LLD law (solid line), to the LLD law with a slip on a length h_p/α (dashed line) and to our model (dotted line). The abrupt fall of h_f shows the existence of a critical capillary number, Ca_c. (*b*) Critical capillary number, Ca_c, below which the textured plate entrains a film of height h_p (the pillar height), as a function of $\alpha^{-3/4}(h_p/a)^{3/2}$, a quantity fixed by the texture design. Circles and squares correspond to experiments with $d = 10$ μm and $d = 20$ μm, and the solid line shows (6), with a numerical coefficient of 1.18.

height, Hasimoto (1959), for example, showed that the increase of friction (i.e. the factor α) can be written as $\alpha - 1 \approx 4\pi h_p^2/(\ln(d/b) - 1.31)d^2$. This formula corrects the scaling observed with h_p and d by a (weak) logarithmic term, including the distance d and the pillar radius b. The coefficient $4\pi/(\ln(d/b) - 1.31)$ is approximately 40 for $d = 10\,\mu$m, larger than the slope in figure 6. However, the flow here is not uniform and the pillars are of finite height, in contrast with Hasimoto's calculation. This should indeed modify the prefactor, which remains to be calculated.

We can finally comment on the regime of constant thickness ($h_d = h_p$, $h_f = 0$). Figure 2 suggests that this regime takes place below a critical capillary number Ca_c, of the order of 10^{-4} in the figure. This observation can be made more quantitative by plotting for the same data the thickness $h_f = h_d - h_p$ of the free layer, as a function of the capillary number (figure 7*a*). Note that h_f follows the LLD law (solid line)

at large thickness, but indeed critically falls (by more than one order of magnitude) around a well-defined capillary number (as observed on a non-wetting plate, yet for a very different reason, by Snoeijer *et al.* 2006). A similar behaviour is expected on a porous plate, which absorbs the entrained liquid. Devauchelle *et al.* (2007) showed that such a critical capillary number also exists when withdrawing a porous plate. A main difference however between this work and our model is that the flow is not exactly known in the case of porous media, which prevents further direct comparison.

More quantitatively, our calculations (dotted line) fit the data for the same value $\alpha = 16.7$. It is worth noticing that modelling the hydrodynamics by just a slip condition at the surface of the trapped layer (with a slip length h_p/α) does not fit the data: rather, the calculated thickness (dashed line) is always above the data, and there is no evidence for a critical capillary number at small Ca (then, the thickness increases as Ca^2 at low Ca). These remarks again emphasize the key role of the flow inside the trapped layer in the limit of small withdrawal velocities.

This critical capillary number can be evaluated in the framework of our model. The dynamic meniscus, whose length scales as $(ah_f)^{1/2}$, matches the flat film (pressure P_o) with the top of the static meniscus (pressure $P_o - \sqrt{2}\gamma/a$): hence, a pressure gradient $\nabla P \sim \gamma/(a^{3/2}h_f^{1/2})$ exists, which induces a flow from the film to the bath. The typical velocity V_p of this flow is given by the Poiseuille law $V_p \sim (h_p^2/\eta_p)\nabla P \sim (\gamma/\eta_p)(h_p^2/a^{3/2}h_f^{1/2})$. If V_p is larger than V, this capillary drainage in the trapped layer is faster than the withdrawal, and a film cannot be entrained above the pillars ($h_f = 0$). This criterion gives a critical capillary number $Ca_c \sim (h_p^2/\alpha a^{3/2}h_f^{1/2})$. For large values of α, h_f should approach the LLD law above Ca_c, which yields

$$Ca_c \sim \alpha^{-3/4}\left(\frac{h_p}{a}\right)^{3/2}. \tag{6}$$

Note that this formula also describes the behaviour expected as α tends to 1. In this limit, we must have $Ca_c \sim (h_p/a)^{3/2}$, i.e. the crossover between the LLD law and the law $h_d = h_p$. We plotted in figure 7(*b*) the measured critical capillary number Ca_c as a function of the dimensionless quantity $\alpha^{-3/4}(h_p/a)^{3/2}$ (6). In this comparison, the value of α is deduced from the fit to the entrainment law (as done in figure 6), for each sample (for which h_p is known). A good agreement with (6) is observed, as shown by the solid line, which also provides a numerical coefficient for the fit of 1.2, of order unity. It is generally of practical interest to increase the domain in capillary number where the film thickness is independent of Ca. Taking the pillar height h_p as the main control parameter, we get from (2) and (6) that Ca_c first increases with h_p (as $h_p^{3/2}$), and then saturates, for $h_p > d$, at a value of the order of $(d/a)^{3/2}$ – hence the recommendation to work with a mutual spacing d comparable to the desired height h_p, in order to make Ca_c as large as possible without having more pillars on the surface than necessary.

4. Conclusions

We have shown how the presence of a well-controlled texture (consisting of micropillars) deeply modifies the quantity of wetting liquid entrained by a moving plate. It was found that the texture thickens the entrained film, compared with what is observed on flat plates. However, it also allows us to 'decide' the thickness of the coating film, independent of the natural coating parameters (velocity, viscosity and surface tension). This property was shown to occur in a large range of capillary

numbers ($0 < Ca < Ca_c$) – a fact of obvious interest in industrial processes where the entrained velocity is often imposed by process constraints, although a particular film thickness is *a priori* desired (for insulation, mechanical, or optical properties). The independence of the thickness of surface tension and viscosity is also valuable, since the coating solutions are likely to age (with a modification of the viscosity) or to contain surfactants or solid particles, which themselves would be likely to influence the film thickness.

We thank M. Reyssat for providing the textured samples and for her help in the reflectometric measurements.

REFERENCES

Afanasiev, K., Munch, A. & Wagner, B. 2007 Landau–Levich problem for non-Newtonian liquids. *Phys. Rev.* E **76**, 036307.

Aradian, A., Raphael, E. & de Gennes, P. G. 2000 Dewetting on porous media with aspiration. *Eur. Phys. J.* E **2**, 367–376.

Beavers, G. S. & Joseph, D. D. 1967 Boundary conditions at a naturally permeable wall. *J. Fluid Mech.* **30**, 197–207.

Bretherton, F. P. 1961 The motion of long bubbles in tubes. *J. Fluid Mech.* **10**, 166–188.

Callies, M., Chen, Y., Marty, F., Pépin, A. & Quéré, D. 2005 Microfabricated textured surfaces for super-hydrophobicity investigations. *Microelectron. Engng* **78–79**, 100–105.

Cazabat, A. M. & Cohen-Stuart, M. A. C. 1986 Dynamics of wetting: effects of surface roughness. *J. Phys. Chem.* **90**, 5845–5849.

Chen, J. D. 1986 Measuring the film thickness surrounding a bubble inside a capillary. *J. Colloid Interface Sci.* **109**, 341–349.

Courbin, L., Denieul, E., Dressaire, E., Roper, M., Ajdari, A. & Stone, H. A. 2007 Imbibition by polygonal spreading on microdecorated surfaces. *Nature Mater.* **6**, 661–664.

Derjaguin, B. 1943 Thickness of liquid layer adhering to walls of vessels on their emptying and the theory of photo- and motion-picture film coating. *Dokl. Acad. Sci. USSR* **39**, 13–19.

Devauchelle, O., Josserand, C. & Zaleski, S. 2007 Forced dewetting on porous media. *J. Fluid Mech.* **574**, 343–364.

Hasimoto, H. 1959 On the periodic fundamental solutions of the Stokes equations and their application to viscous flow past a cubic array of spheres. *J. Fluid Mech.* **5**, 317–328.

Ishino, C., Reyssat, M., Reyssat, E., Okumura, K. & Quéré, D. 2007 Wicking within forest of micro-pillars. *EPL* **79**, 56005.

Jäger, W. & Mikelic, A. 2000 On the interface boundary condition by Beavers, Joseph and Saffman. *SIAM J. Appl. Mech.* **60**, 1111–1127.

Krechetnikov, R. & Homsy, G. M. 2005 Experimental study of substrate roughness and surfactant effects on the Landau–Levich law. *Phys. Fluids* **17**, 102108.

Landau, L. & Levich, V. 1942 Dragging of a liquid by a moving plate. *Acta Physicochim. USSR* **17**, 42–54.

Maleki, M., Reyssat, M., Restagno, F., Quéré, D. & Clanet, C. 2011 Landau–Levich menisci. *J. Colloid Interface Sci.* **354**, 359–363.

McHale, G., Shirtcliffe, N. J., Aqil, S., Perry, C. C. & Newton, M. I. 2004 Topography driven spreading. *Phys. Rev. Lett.* **93**, 036102.

Ramdane, O. O. & Quéré, D. 1997 The thickening factor in Marangoni coating. *Langmuir* **13**, 2911–2916.

Savva, N., Kalliadasis, S. & Pavliotis, G. A. 2010 Two-dimensional droplet spreading over random topographical substrates. *Phys. Rev. Lett.* **104**, 084501.

Shen, A. Q., Gleason, B., McKinley, G. H. & Stone, H. A. 2002 Fiber coating with surfactant solutions. *Phys. Fluids* **14**, 4055–4068.

Snoeijer, J. H., Delon, G., Fermigier, M. & Andreotti, B. 2006 Avoided critical behavior in dynamically forced wetting. *Phys. Rev. Lett.* **96**, 174504.